Electronic Supplementary Information

Ultra-Efficient Electrocatalytic Hydrogen Evolution at One-Step Carbonization Generated Molybdenum Carbide Nanosheets/N-doped Carbon

Cuicui Du,[a] Hao Huang,[a] Yue Wu,[a] Siyuan Wu[a] and Wenbo Song[a]*

[a.]College of Chemistry, Jilin University, Changchun 130012, P.R. China

E-mail: wbsong@jlu.edu.cn Fax: +86-431-85168420.

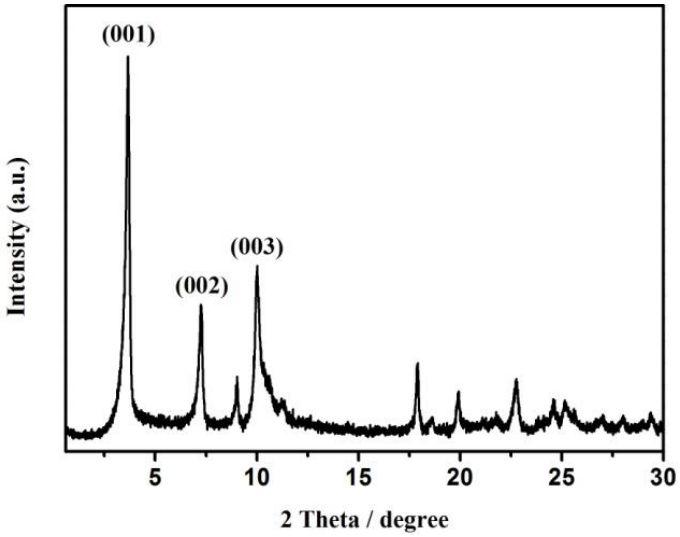

Fig. S1 The XRD pattern for Mo-LM precursor fitting with the reference[1].

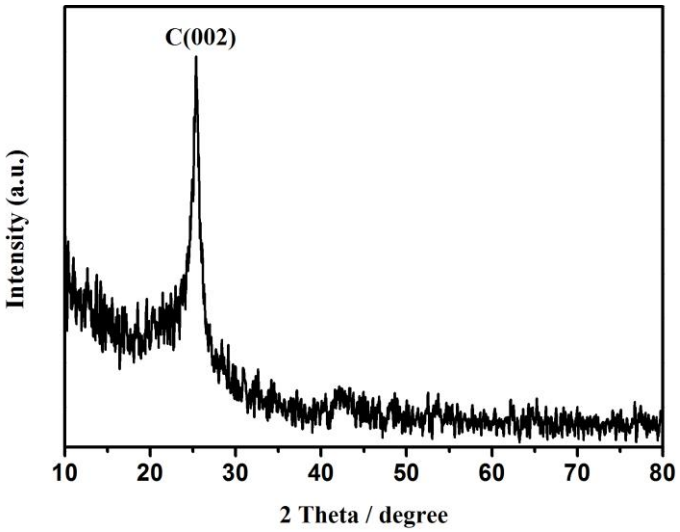

Fig. S2 The XRD pattern of N-doped carbon with diffraction peak at 2θ =25.3° assigned to the (002) plane of graphitic carbon.

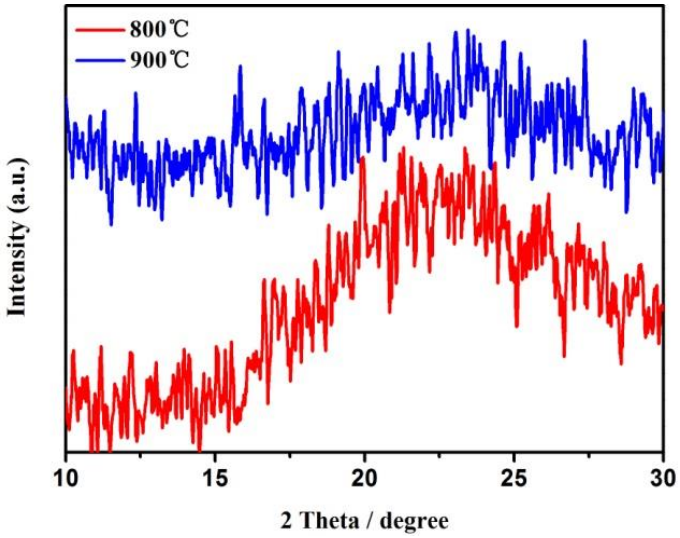

Fig. S3 The zoom-in XRD patterns for MCNS/NC annealed at 800°C and 900°C.

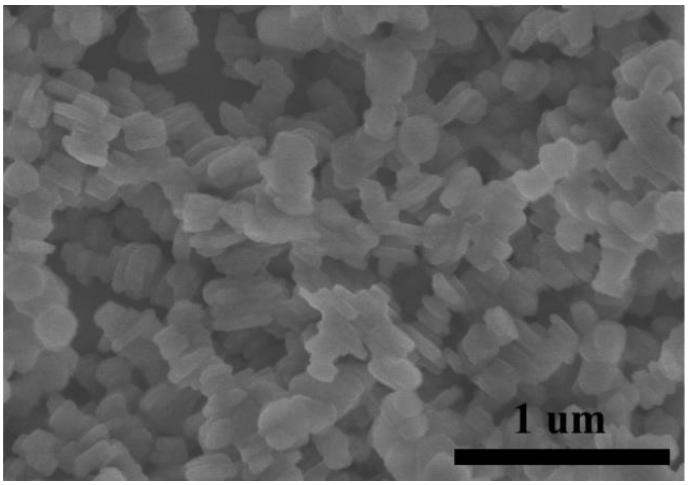

Fig. S4 The SEM image of Mo-LM hybrid precursor.

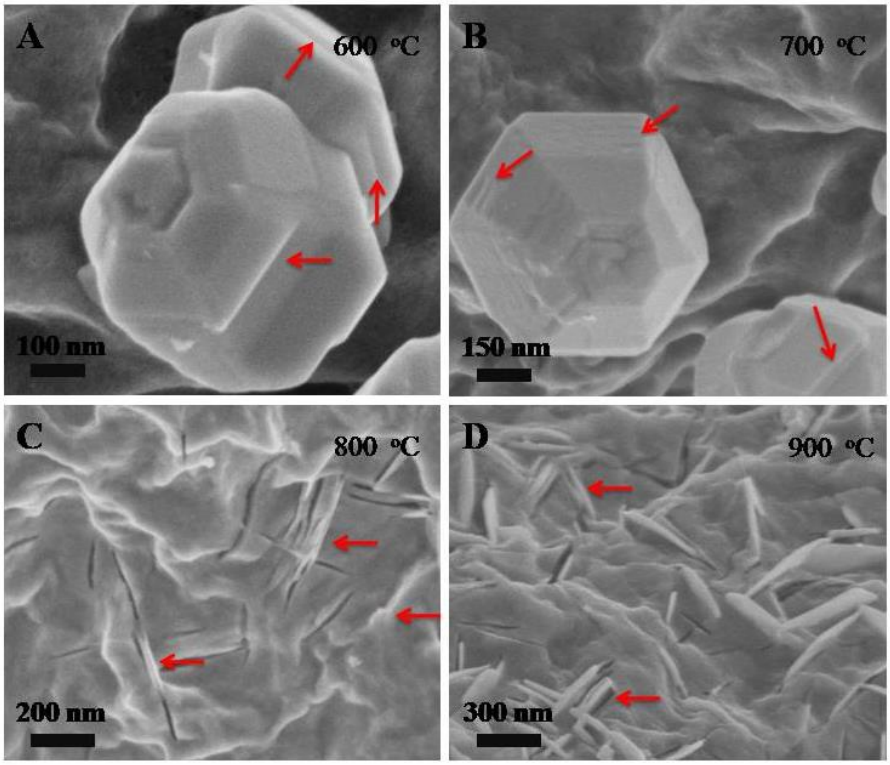

Fig. S5 The SEM images of the samples obtained at different temperature.

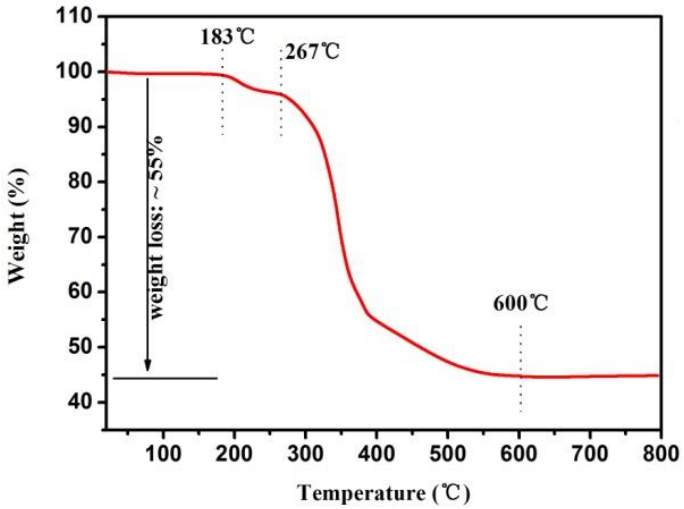

Fig. S6 The TGA curve of Mo-LM hybrid precursor measured from 20 to 800°C in nitrogen atmosphere with a heating rate of 10°C min^{-1}.

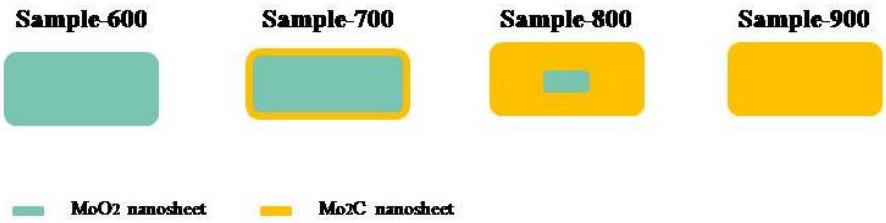

Fig. S7 The temperature-dependent structure evolution of the Mo-based nanosheet.

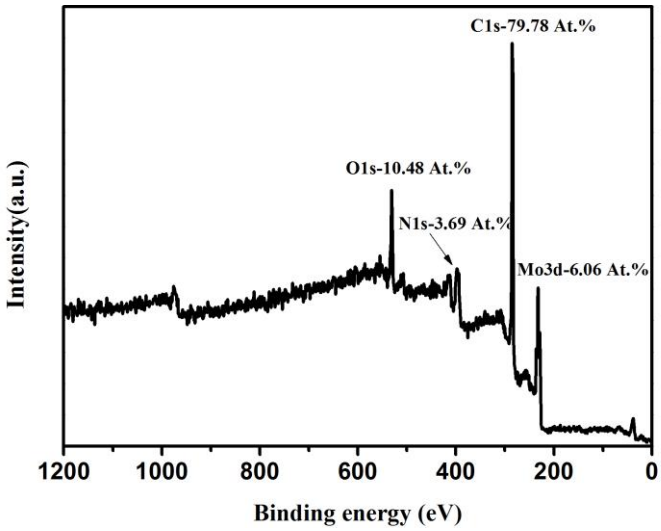

Fig. S8 The XPS spectrum of MCNS/NC.

For the TGA curve, the initial weight gain below 380 °C is ascribed to the oxidation of Mo_2C to MoO_3, followed by the gradual combustion of carbon with further increasing temperature, manifesting approximate 7.5% weight loss. The remaining weight of the sample after heating to 520°C is about 92.5 wt.%. Therefore, the carbon content could be calculated from the following equation:

$$w\ (carbon) = 1 - 92.5\ wt.\% * M(Mo_2C)/2M(MoO_3) = 34.5\ wt.\%.$$

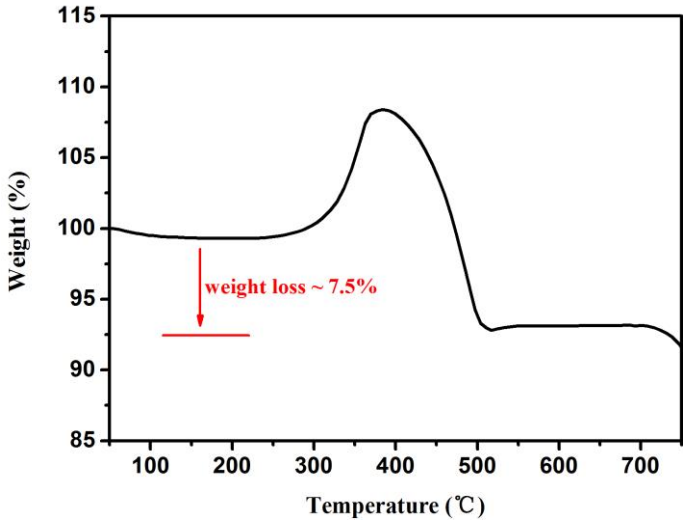

Fig. S9 TGA curve of the as-prepared MCNS/NC from 50 to 750 °C under air gas with a temperature ramp of 10 °C min^{-1}.

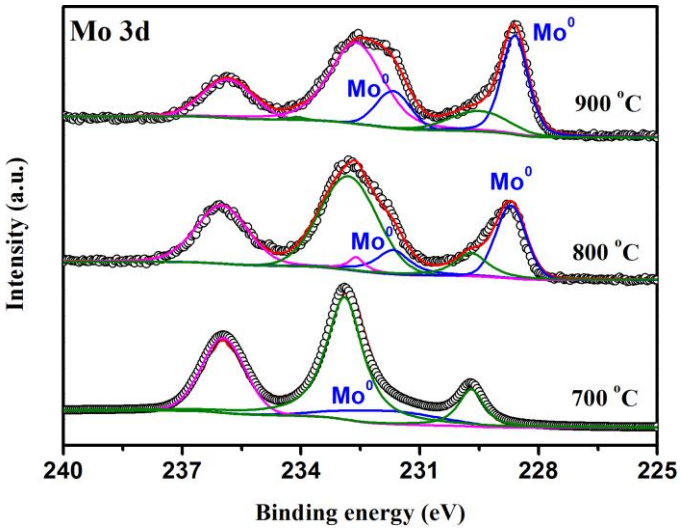

Fig. S10 The high-resolution XPS spectra of Mo 3d for series samples obtained at different annealing temperature (the blue curves represent the peaks of Mo^0).

Based on the "outside-in" carburization mechanism, the structure of the nanosheets obtained at different temperature can be represented in Fig. S7. Despite of the different surface layer thickness of Mo_2C on samples of 700, 800 and 900 ^oC, the effective electroactive surface areas of sample-700 and 800 (estimated from the electrochemical double layer capacitance measurement in Fig. S14) are very similar. Since the effective electrochemical active surface of a catalytic material plays a key role in HER catalysis, the sample-700 and 800 may display similar HER activity. The sample of 900 ^oC exhibits an increase of effective electroactive surface area, which may lead to enhanced HER activity.

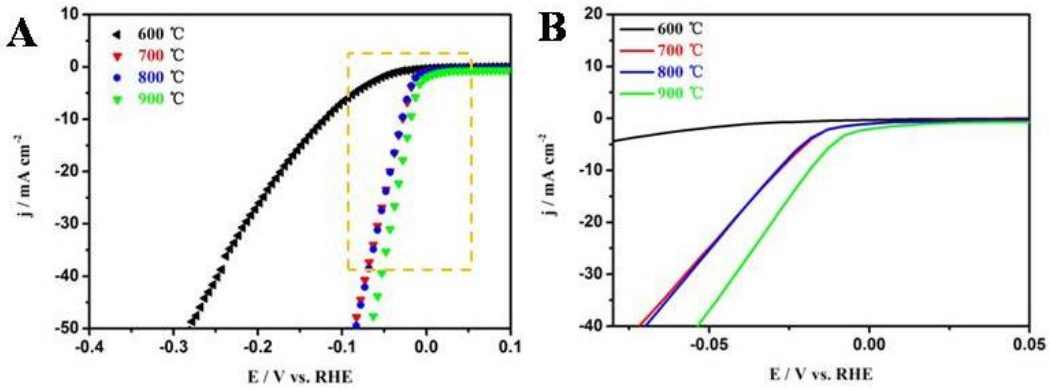

Fig. S11 (A) The polarization curves and (B) the corresponding zoom-in graph of series of samples prepared at different temperature.

On the basis of LSV in Fig. S11, the linear fit using the Tafel equation for Sample-700, Sample-800 and Sample-900 yields an apparent Tafel slope of 30.6, 30.1, and 28.9 mV dec^{-1} respectively (Fig. S12), which are much smaller than that of Sample-600. This result implies an accelerated rate for HER along with the generation of Mo_2C.

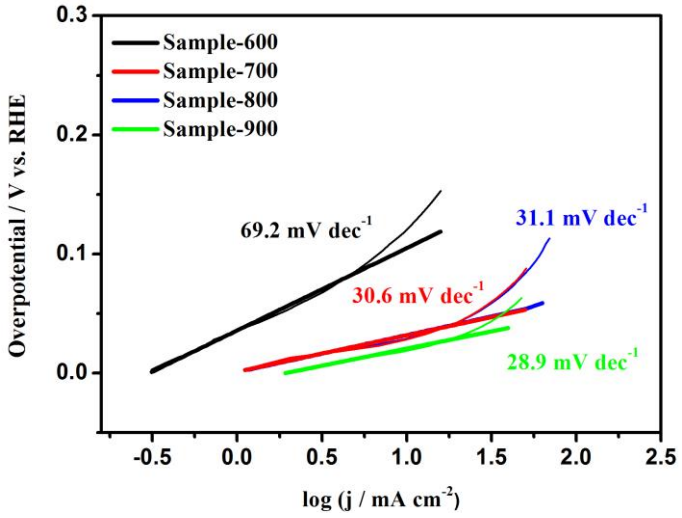

Fig. S12 Tafel plots of Sample-600, Sample-700, Sample-800 and Sample-900.

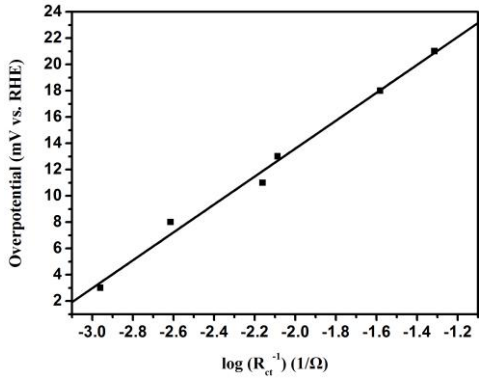

Fig. S13 The plot of overpotential versus log (R_{ct}^{-1}) fitted from EIS data.

The electrochemical double-layer capacitance calculation:

The electrochemical double layer capacitance (C_{dl}) was determined from the CVs measured in a non-Faradaic region at different scan rates (v). The scan rates were chosen from 5 to 200 mV s^{-1}. The total current at +0.2 V vs. RHE is plotted against the scan rate, which was obtained from the addition of the absolute values in the cathodic and anodic wave. The slope of each curve is twice the value of C_{dl}.

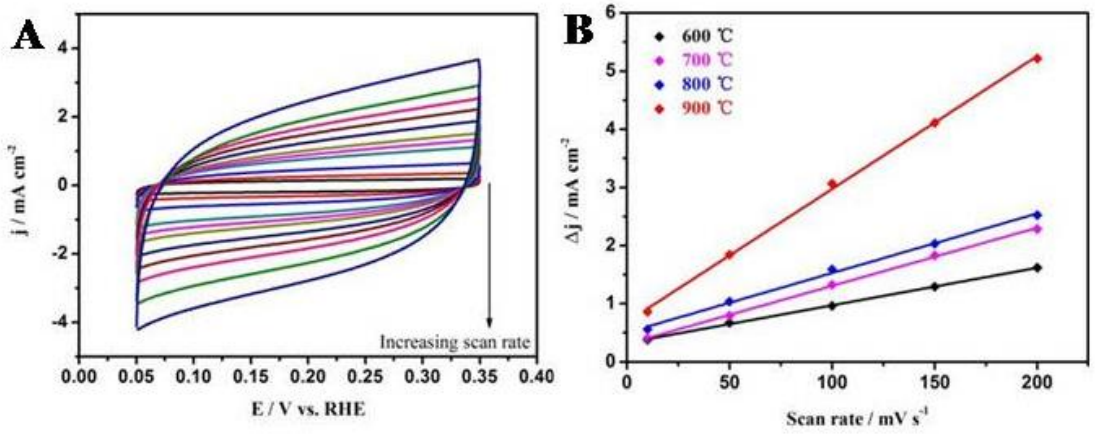

Fig. S14 Electrochemical capacitance measurements. (A) CV curves of MCNS/CN measured from 5 to 200 mV s^{-1} and (B) comparative plots of *Δj* versus scan rate fitted from CV curves at +0.2 V vs. RHE for MCNS/CN with the other samples obtained at lower temperature.

Electrochemical impedance spectroscopy (EIS) is a powerful technique in the characterization of interfacial reactions and electron-transfer kinetics in HER. Fig. S15 shows similar Nyquist plots for Sample-700, Sample-800 and Sample-900. The charge transfer resistance (R_{ct}) of Sample-900 is slightly smaller than Sample-800 and Sample-700. Particularly, different from Sample-700 and Sample-800, two semicircles present on the Nyquist plot of Sample-900, and the higher frequency one relates to the surface porosity.[25-27] The slightly improved electrocatalytic activity of Sample-900 than the others could thus be ascribed to good accessibility as well as enhanced conductivity due to increased graphitization degree of the carbon matrix.

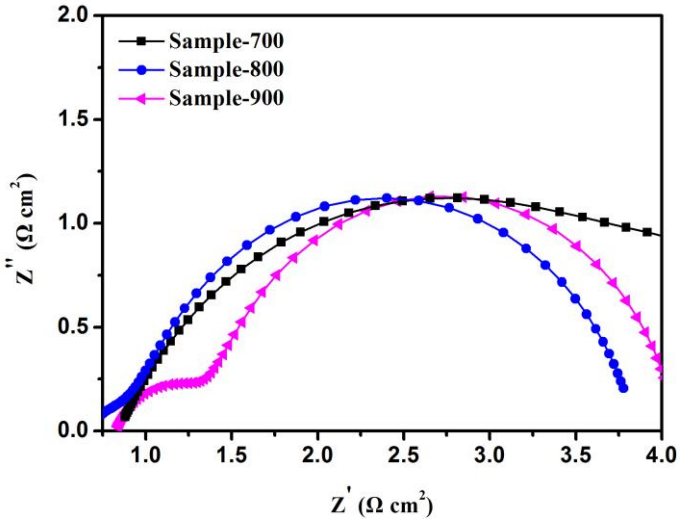

Fig. S15 Comparative Nyquist plots of series samples obtained at different annealing temperature at overpotential of 18 mV.

The stability of Sample-700 and Sample-800 in acidic environment was also evaluated by collecting the current–time plot at an applied overpotential of 38mV (vs. RHE). It can be seen from Fig. S16 that the reduction current of Sample-800 remains fairly stable 14 h of continuous operation, indicating relative durability of the electrode for HER in 0.5 M H_2SO_4. However, an apparently current loss was observed for Sample-700, since MoO_2 is reported to be less stable in the acidic electrolyte.[28]

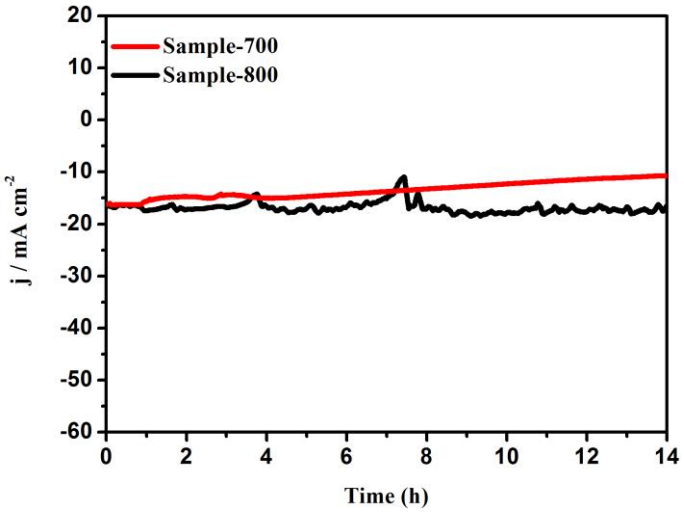

Fig. S16 Current–time plots for Sample-700 and Sample-800 at an overpotential of 38mV (vs.RHE) in acidic electrolyte.

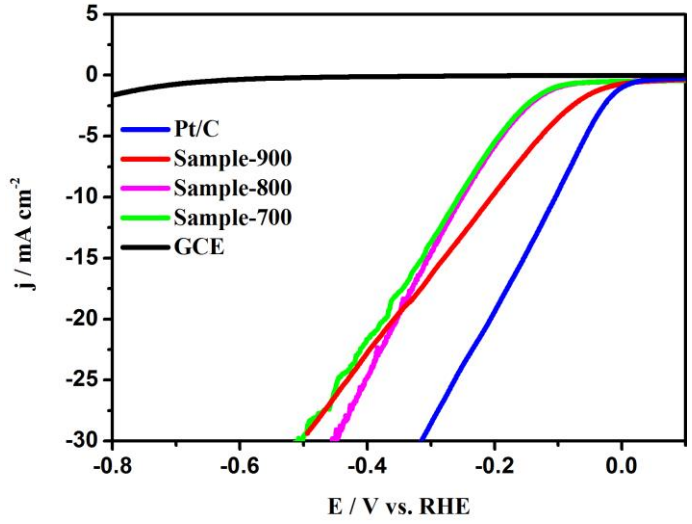

Fig. S17 Linear sweep voltammetry curves of Sample-700, Sample-800, Sample-900, GCE and Pt/C for HER in 0.1M KOH.

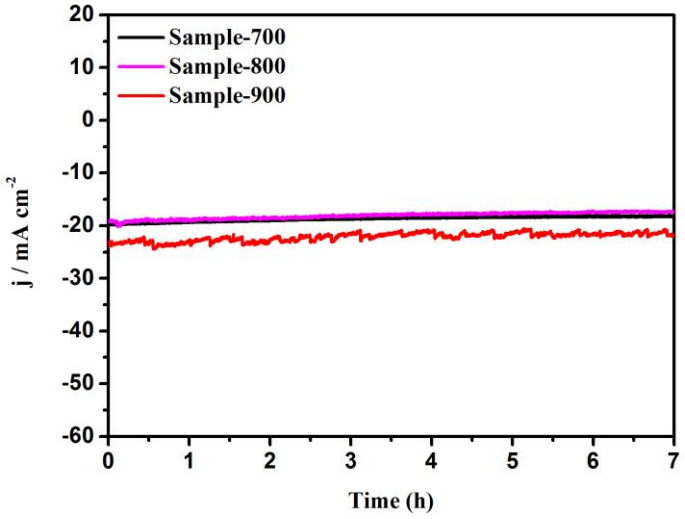

Fig. S18 The time-dependent current density of Sample-700, Sample-800 and Sample-900 in 0.1M KOH at the overpotential of ~360 mV, ~340 mV and ~400 mV (vs. RHE), respectively.

Table S1. The comparative HER performances of MCNS/NC and other catalyts.

[ref] Catalyst [mg cm^{-2}]	Electrolyte	Onset overpotential [mV]	Overpotential @ 10 mA cm^{-2} [mV]	Tafel slope [mV dec^{-1}]
[2]CoNi @NC (0.32)	0.1 M H_2SO_4	0	140	104
[3]$Ni_{0.33}Co_{0.67}S_2$ (—)	0.5 M H_2SO_4	65	—	44
	1 M KOH	50	88	118
[4]CoP/CNT (0.285)	0.5 M H_2SO_4	40	122	54
[5]Co–W carbide NPs (0.28)	1 M KOH	26	73	25
[6] MoP (0.86)	0.5 M H_2SO_4	50	135	54
[7]Mo_2C/CNT (2)	0.1M $HClO_4$	63	149	55.2
[8]MoS_2/CNTs (0.136)	0.5 M H_2SO_4	90	184	44.6
[9]WS_2 nanosheets (0.285)	1 M H_2SO_4	60	151	72
[10] NiAu alloy NPs (0.2)	0.5 M H_2SO_4	~ 7	—	36
[11]SCEIN/SWNT (0.18)	0.5 M H_2SO_4	~ 0	77	40
[12]SnS/N-rGr (0.28)	0.5 M H_2SO_4	59	130	38
[13] P-WN/rGO (0.337)	0.5 M H_2SO_4	46	85	54
[14] Pt-CNSs/RGO (0.078)	0.5 M H_2SO_4	18	~ 75	29
[15] $NiSe_2$ nanoparticles (1)	0.5 M H_2SO_4	—	170	31.1
[16] Ni_2P nanoparticles (—)	0.5 M H_2SO_4	20	—	75
[17]MoP microparticles (0.1)	0.5 M H_2SO_4	80	150	50
[18]iron-nickel sulfide (0.254)	0.5 M H_2SO_4	—	105	40
[19]FeP-CS (0.28)	0.5 M H_2SO_4	38	112	58
[20] $Fe_{1-x}Co_xS_2$/CNT (0.4)	0.5 M H_2SO_4	90	—	46
[21]MoC_x (0.8)	0.5 M H_2SO_4	~ 25	142	53
	1 M KOH	~ 80	151	59
[22] Mo_2C–NCNTs (~3)	0.5 M H_2SO_4	72	147	71
	1 M KOH	—	257	—
[23]Mo_2C–RGO (0.285)	0.5 M H_2SO_4	~ 70	130	54
[24]$CoSe_2$ nanosheet (0.142)	0.1 M KOH	—	320	44
[this work] MCNS/NC	0.5 M H_2SO_4	~ 0	19	28.9
	0.1 M KOH	24	205	140

References

1 W. Han, P. Yuan, Y. Fan, H. Y. Liu and X. J. Bao, *J. Mater. Chem.*, 2012, **22**, 12121.

2 J. Deng, P. J. Ren, D. H. Deng and X. H. Bao, *Angew. Chem. Int. Edit.*, 2015, **54**, 2100.

3 Z. Peng, D. S. Jia, A. M. Al-Enizi, A. A. Elzatahry and G. F. Zheng, *Adv. Energy. Mater.*, 2015, **5**, 1402031.

4 Q. Liu, J. Q. Tian, W. Cui, P. Jiang, N. Y. Cheng, A. M. Asiri and X. P. Sun, *Angew. Chem. Int. Edit.*, 2014, **53**, 6710.
5 Y. P. Liu, G. D. Li, L. Yuan, L. Ge, H. Ding, D. J. Wang and X. X. Zou, *Nanoscale*, 2015, **7**, 3130.
6 P. Xiao, M. A. Sk, L. Thia, X. M. Ge, R. J. Lim, J. Y. Wang, K. H. Lim and X. Wang, *Energ. Environ. Sci.*, 2014, **7**, 2624.
7 W. F. Chen, C. H. Wang, K. Sasaki, N. Marinkovic, W. Xu, J. T. Muckerman, Y. Zhu and R. R. Adzic, *Energ. Environ. Sci.*, 2013, **6**, 943.
8 Y. Yan, X. M. Ge, Z. L. Liu, J. Y. Wang, J. M. Lee and X. Wang, *Nanoscale*, 2013, **5**, 7768.
9 Z. Z. Wu, B. Z. Fang, A. Bonakdarpour, A. K. Sun, D. P. Wilkinson and D. Z. Wang, *Appl. Catal. B-Environ.*, 2012, **125**, 59.
10 H. F. Lv, Z. Xi, Z. Z. Chen, S. J. Guo, Y. S. Yu, W. L. Zhu, Q. Li, X. Zhang, M. Pan, G. Lu, S. C. Mu and S. H. Sun, *J. Am. Chem. Soc.*, 2015, **137**, 5859.
11 M. Tavakkoli, T. Kallio, O. Reynaud, A. G. Nasibulin, C. Johans, J. Sainio, H. Jiang, E. I. Kauppinen and K. Laasonen, *Angew. Chem. Int. Edit.*, 2015, **54**, 4535.
12 S. S. Shinde, A. Sami, D. H. Kim and J. H. Lee, *Chem. Commun.*, 2015, **51**, 15716.
13 H. J. Yan, C. G. Tian, L. Wang, A. P. Wu, M. C. Meng, L. Zhao and H. G. Fu, *Angew. Chem. Int. Edit.*, 2015, **54**, 6325.
14 G. R. Xu, J. J. Hui, T. Huang, Y. Chen and J. M. Lee, *J. Power Sources*, 2015, **285**, 393.
15 J. Liang, Y. C. Yang, J. Zhang, J. J. Wu, P. Dong, J. T. Yuan, G. M. Zhang and J. Lou, *Nanoscale*, 2015, **7**, 14813.
16 J. S. Moon, J. H. Jang, E. G. Kim, Y. H. Chung, S. J. Yoo and Y. K. Lee, *J Catal*, 2015, **326**, 92.
17 T. Y. Wang, K. Z. Du, W. L. Liu, Z. W. Zhu, Y. H. Shao and M. X. Li, *J. Mater. Chem. A*, 2015, **3**, 4368.
18 X. Long, G. X. Li, Z. L. Wang, H. Y. Zhu, T. Zhang, S. Xiao, W. Y. Guo and S. H. Yang, *J. Am. Chem. Soc.*, 2015, **137**, 11900.
19 Z. Zhang, J. H. Hao, W. S. Yang, B. P. Lu and J. L. Tang, *Nanoscale*, 2015, **7**, 4400.
20 D. Y. Wang, M. Gong, H. L. Chou, C. J. Pan, H. A. Chen, Y. P. Wu, M. C. Lin, M. Y. Guan, J. Yang, C. W. Chen, Y. L. Wang, B. J. Hwang, C. C. Chen and H. J. Dai, *J. Am. Chem. Soc.*, 2015, **137**, 1587.
21 H. B. Wu, B. Y. Xia, L. Yu, X. Y. Yu and X. W. Lou, *Nat. Commun.*, 2015, **6,** 6512.
22 K. Zhang, Y. Zhao, D. Y. Fu and Y. J. Chen, *J. Mater. Chem. A*, 2015, **3**, 5783.
23 L. F. Pan, Y. H. Li, S. Yang, P. F. Liu, M. Q. Yu and H. G. Yang, *Chem. Commun.*, 2014, **50**, 13135.
24 Y. Liu , H. Cheng, M. Lyu, S. Fan, Q. Liu, W. Zhang, Y. Zhi, C. Wang, C. Xiao, S. Wei, B. Ye, Y. Xie, *J. Am. Chem. Soc.,* 2014, **136**, 15670.
25 Y. P. Zhu, Y. P. Liu, T. Z. Ren and Z. Y. Yuan, *Adv. Funct. Mater.*, 2015, **25**, 7337.
26 L. Liao, S. N. Wang, J. J. Xiao, X. J. Bian, Y. H. Zhang, M. D. Scanlon, X. L. Hu, Y. Tang, B. H. Liu and H. H. Girault, *Energ. Environ. Sci.*, 2014, **7**, 387.
27 L. Ma, L. R. L. Ting, V. Molinari, C. Giordano and B. S. Yeo, *J. Mater. Chem. A*, 2015, **3**, 8361.
28 L. J. Yang, W. J. Zhou, D. M. Hou, K. Zhou, G. Q. Li, Z. H. Tang, L. G. Li and S. W. Chen, *Nanoscale*, 2015, **7**, 5203-5208.